



Removing of Sb and As from Electrolyte in Copper Electrorefining Process: A Green Approach

M. R. Shojaei^a, G. R. Khayati^{*b}, N. Assadat Yaghubi^c, F. Bagheri Sharebabaki^d, S. M. J. Khorasani^e

^a Department of Materials Science and Engineering, Sharif University of Technology, Tehran, Iran

^b Department of materials science and Engineering, Shahid Bahonar University of Kerman, Kerman, Iran

^c Research & Development Center, Shahrabak Copper Complex, National Iranian Copper Industries Company, Kerman, Iran

^d Supervisor of Copper Electrorefining Operation, Khatoonabad copper refinery, Shahrehabak copper complex, National Iranian copper industries company, Kerman, Iran

^e Senior metallurgical engineer, Process control unit, Khatoonabad copper refinery, Shahrehabak copper complex, National Iranian copper industries company, Kerman, Iran

PAPER INFO

Paper history:

Received 08 August 2020

Received in revised form 26 September 2020

Accepted 29 October 2020

Keywords:

Antimony

Arsenic Copper

Cooling

Electrorefining

ABSTRACT

Removing of arsenic and antimony from electrolyte of copper electrorefining plant by cooling treatment is the subject of current study. In this regards, the temperature of various electrolyte samples reduce to 5, 10, 15 and 20 °C and hold at different times without any turbulency. Experimental results reveal that decreasing the temperature of the electrolyte, facilitate the deposition of As and Sb in the form of AsO₅Sb, AsO₄Sb and As₂O₃ as the white precipitate at a critical time. Also, in the case of the electrolyte retention times exceed than the critical time, the copper content of electrolyte precipitate as blue phase. Typically, it is possible to remove 27 wt.% of Sb and 6 wt.% of As by the cooling of the electrolyte to 5 °C after 8 h. It seems that due to the biocompatibility, the lack of need to the complex technology and its simplicity, the proposed method is a suitable alternative to the common approaches for the removal of antimony and arsenic from industrial electrolyte.

doi: 10.5829/ije.2021.34.03c.14

1. INTRODUCTION

Electrorefining is one of the most common technique in which the high quality of copper cathode (99.99 wt.%) is produced. In this technique, impure copper cast anodes (about 98.5 wt.%) uses as the source of copper and dissolve electrochemically in H₂SO₄ solution as the electrolyte. Then, the Cu ions selectively electrodeposited on the stainless steel cathode blanks. The impurities in the electrorefining cell can be categorized into two groups:

(i) Au, Os, Ru, Ir, Rh, Pd, Pt, Pb, Te, Se and Sn with a negligible tendency for dissolution in the electrorefining cell. These impurities are not electrodeposited at the stainless cathode blank and in the ideal condition go to the anodic slimes;

(ii) Sb, Bi, As, S, Fe, Co and Ni that dissolve in the electrolyte with the significant tendency for dissolution in the electrolytes.

Due to the deposition of copper at lower potentials than type (ii), these impurities accumulate in the electrolyte. In these conditions fail to remove these impurities from the electrolyte has a detrimental effect on the purity of the cathode produced. As a result, these impurities must be continuously removed from the electrolytes, [1].

Historically, As and Sb have been recognized as two of the most challenging impurities in the copper electrorefining. Typically, the former segregates at the grain boundary and deteriorate the mechanical properties of copper through the drawing. While, the later causes the nodulation of the cathode, lowering of current efficiency and passivation [2, 3]. In this regard, the removal of As and Sb is a hot issue with the significant desirability in

*Corresponding Author Email: mohammadrezashojaei3@gmail.com
(M. R. Shojaei)

the copper electrorefining plants. Numerous methods have been introduced to remove As and Sb from electrorefining copper plants, including the bleeding of electrolyte that strongly dependent on the location of the electrorefining plant [4], usage of liberator cells [3], ion exchange [4], adding the removal agents [5], using of the organic phase by solvent extraction [6], absorption by activated carbon [6], co-precipitation of Bi and Sb by adding of barium or lead carbonates [7], crystallization of As with SO_2 [8], removal of Sb and Bi by titanium (IV) oxysulfate co-precipitation [9] and self-purification of copper electrolyte [10]. To the best of our knowledge, all of above methods are complicated and finding of an eco-friendly way to remove As and Sb from the electrolyte is strongly appreciated. This paper is an attempt to remove As and Sb with a green method to reduce the energy consumption and costs. As a first report, in this paper, a simple method is proposed for the removal of As and Sb ions from the electrolyte of the copper electrorefining plants in the industrial scale.

2. EXPERIMENTAL

The industrial electrolyte (mother sample) is selected from the output of the polishing filter of Khatoon Abad industrial company in Shahrabak, Iran. It is free of suspended and floating slimes and reflects the actual behavior of electrolyte through the cooling treatment. It is necessary to note that the amount of Bi in Sarcheshmeh mine is too low (10-20 ppm). Also, the additives including leveling agent and grain refining agent animal glue and thiourea at the electrolyte have no effect on the removal of As and Sb due to dissociation after about 120 min [11-12]. Since the mole fraction of As/(Bi+Sb) in casting anode of a selected plant is higher than 4, it is possible to provide the possibility of self-purification and caused the errors in the results. Accordingly, the mother sample is held for 24 h in 62°C (i.e., the operational temperature of the electrorefining plant) as a first step. Then, four samples selected and cooled until 5, 10, 15, and 20°C , separately in an incubator (Hanchen Model: ES-60). Figure 1 shows schematic steps of the proposed method for removing the impurities. To determine the critical time required for the removal of arsenic and antimony, all samples were allowed to form a white precipitate (its constituents are As, Sb and O) in selected cooling temperature. It is important to note all samples are quite stagnant until the formation of white precipitate is completed. Also, to determine the critical times for the crystallization of CuSO_4 as a blue precipitate, the cooling process is continued until the crystallization has occurred on the white precipitate. Collected precipitates are washed four times with deionized water and then dried at 50°C for 60 min. Each experiment is repeated three times and 10 mL of each sample is selected and mixed to make the sample for chemical analysis. A scanning electron

microscope (SEM, VGA, TESCAN, XMU) at 20KV as an accelerating voltage equipped with an EDS detector is used to analyze the chemical component of the precipitates. The X-ray diffraction (XRD) pattern is recorded by Rigaku mini flex diffractometer with Cu-K α X-ray diffraction at 35 kV and 20 mA. The vibration characteristic is determined by IR spectroscopy (Nexus 670, Nicolet crop). ANALYAST DIVISION: WET, AAS, ELECTRO ANALYSE are also employed for chemical analysis of selected electrolytes before and after the cooling treatment.

The density functional theory calculations are performed utilizing the CP2K software package [13]. Double ζ -valence polarized basis set [14], Perdew-Burke-Ernzerhof generalized gradient approximation exchange-correlation functional [15], and Goedecker-Teter-Hutter pseudopotential [16] are used for self-consistent field (SCF) calculations. The charge density cutoff radius of 300 Ry with the convergence limit of 10^{-6} is adopted. The geometries are optimized until the force on each atom is less than $15\text{ meV}/\text{\AA}$ with a maximum displacement of 0.002 Bohr using the Broyden-Fletcher-Goldfarb-Shanno algorithm [17]. For calculation of the normal modes of the vibrations, the geometries are further optimized until the force on each atom is less than $1\text{ meV}/\text{\AA}$. The convergence criterion for SCF calculations is set to 10^{-8} . The structures and the isosurfaces of molecular orbitals are shown using a piece of VESTA software [17].

3. RESULTS AND DISCUSSION

3.1. Selected Cooling Cycles

To determine the critical time for the formation of the white precipitate and crystallization of blue copper sulfates, each sample is kept at the selected temperature until the blue copper sulfates is formed as reported in Table 1. As a first result, there is a significant difference between the critical time

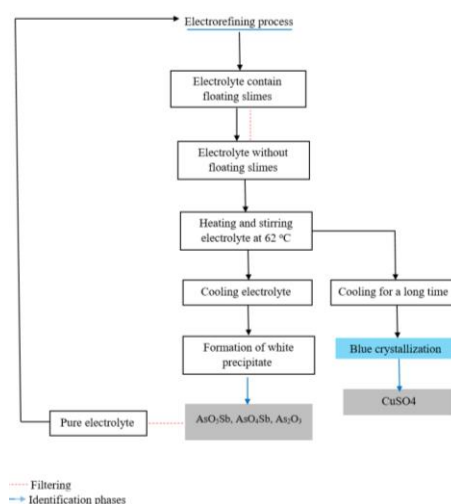


Figure 1. Schematic presentation of the proposed method for the removal of As, Sb

TABLE 1. Temperature and critical time for the precipitation of white and blue type in various samples

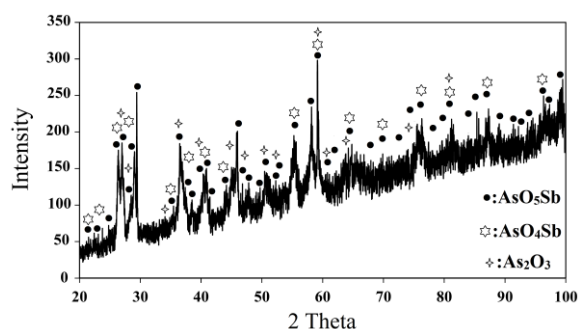
Temperature (°C)	5	10	15	20
Minimum time required for the formation of a white precipitate (h)	8	11	14	16
Minimum time required for the crystallization of copper sulfate as a blue precipitate (h)	12	15	20	24

of the formation of white precipitate and the crystallization of the copper sulfate at the selected cooling temperatures. Typically, this difference from 3 h at 2 °C enhanced to the about 8 h at 20 °C for the formation of white precipitate. The critical times increases at higher temperature for the storage of the electrolyte. Therefore, compared to the temperature, the super saturation due to the decrease in temperature is the administrated factor on the formation of white precipitate. In other words, the higher the degree of saturation is performed at a lower temperature. It is also possible to selectively separate the two phases over a relatively long time for all investigated temperatures.

3. 2. Phase and Structural Analysis of Collected White Precipitates

The phase analysis of a white precipitate is carried out using XRD. All samples showed similar XRD patterns. Figure 2 typically shows the XRD pattern of white precipitate from cooled electrolyte for 8 h at 5 °C. As shown, AsO_5Sb (PDF: 98-001-6465), As_2O_3 (PDF no. 01-083-1548) and AsO_4Sb (PDF no.: 73-0875), respectively are the main phases with relatively crystalline characteristics. Peak broadening can be related to the amorphous characteristics of these phases and/or the ultra-fine particles size of the precipitate. Also, the weight percent of other possible impurities in white precipitates is lower than 5 wt.% and as a consequence there is not any peaks of these impurities.

Figure 3(a) typically illustrates the SEM image (using a backscatter detector) of collected white precipitates after the storage of electrolyte at 5 °C for 8 h.

**Figure 2.** Typically, the XRD pattern of white precipitate after the cooling of electrolyte at 5 °C for 8 h

Accordingly, the presence of three various morphologies including plate-like, rod-like and spherical is obvious. As shown, the sizes of spherical particles are lower than 500 nm and may be one of the reasons of peak broadening in the XRD pattern. Also, due to the different average atomic mass units of observed phases in the XRD pattern ($\text{Amu}_{\text{AsO}_5\text{Sb}}=39.5$, $\text{Amu}_{\text{As}_2\text{O}_3}=39.6$ and $\text{Amu}_{\text{AsO}_4\text{Sb}}=43.5$), it can be concluded that the brighter spherical particles are related to AsO_4Sb due to the higher average atomic mass unit. In this regard, the similar brightness of rod-like and plate-like particles can be related to a similar average atomic mass unit of these phases. The EDS is used to determine the chemical composition of A, B and C points in Figures 3(b), 3(c) and 3(d). As can be seen from the EDS spectrum of point A, As, Sb and O are the main constituents of selected flake particles. Similar elements are also observed in the EDS spectrum of point C at the surface of rod-like particles. While, at the EDS of point B (Figure 3(c)), instead of Sb, there are some minor amounts of Cu and S due to the entrapment of electrolyte at the surface crack of rod-like particles.

To further investigate of these phases, the chemical analysis of electrolyte is determined before and after the cooling and the formation of a white precipitate. Table 1 typically, compares the chemical composition of as received and cooled electrolyte to 5 °C for 8 h.

As the first conclusion of Table 2, the content of Ni, Cu, Bi, Co and Fe are relatively constant for both the electrolytes and strongly rejected the co-precipitation of these ions through the cooling. The concentration of As(III) and Sb(III) experience little change including 0.03 g/L and 0.03 g/L, respectively. While, the maximum decrease in the concentration related to the As(V) and Sb(V) to be about 0.23 g/L and 0.09 g/L after the cooling, respectively.

3. 3. Mechanism of the Removal of Antimony and Arsenic from Electrolyte

The phase analysis of precipitates confirms the presence of crystalline AsO_5Sb , AsO_4Sb and As_2O_3 phases. As shown in Table 2, As(V), As(III), Sb(V), Sb(III) are the main constituents that change their concentration after the cooling. According to the literature, H_3AsO_4 , $\text{AsO}^+/\text{HAsO}_2$, HSb(OH)_6 and SbO^+ are the stable component of these components in the electrolyte [18]. Given that, the pressure, acidity and type of electrolytes are not changed through the cooling. It can be concluded that the temperature has a key role in the ratio of As(V)/As(III) and Sb(V)/Sb(III) through the cooling. An increase in As(III) after the cooling cycle, despite the decrease in As(V), Sb(III) and Sb(V) contents is the other notable concept in Table 1. Ying-Lin Peng et al. [19] showed that the oxidation of As(III) to As(V) facilitates at the higher temperature. They reported that at constant electrolysis time of 168 h, the oxidation rates of As(III) from As(V) at the temperature 75 °C is 2.21 times

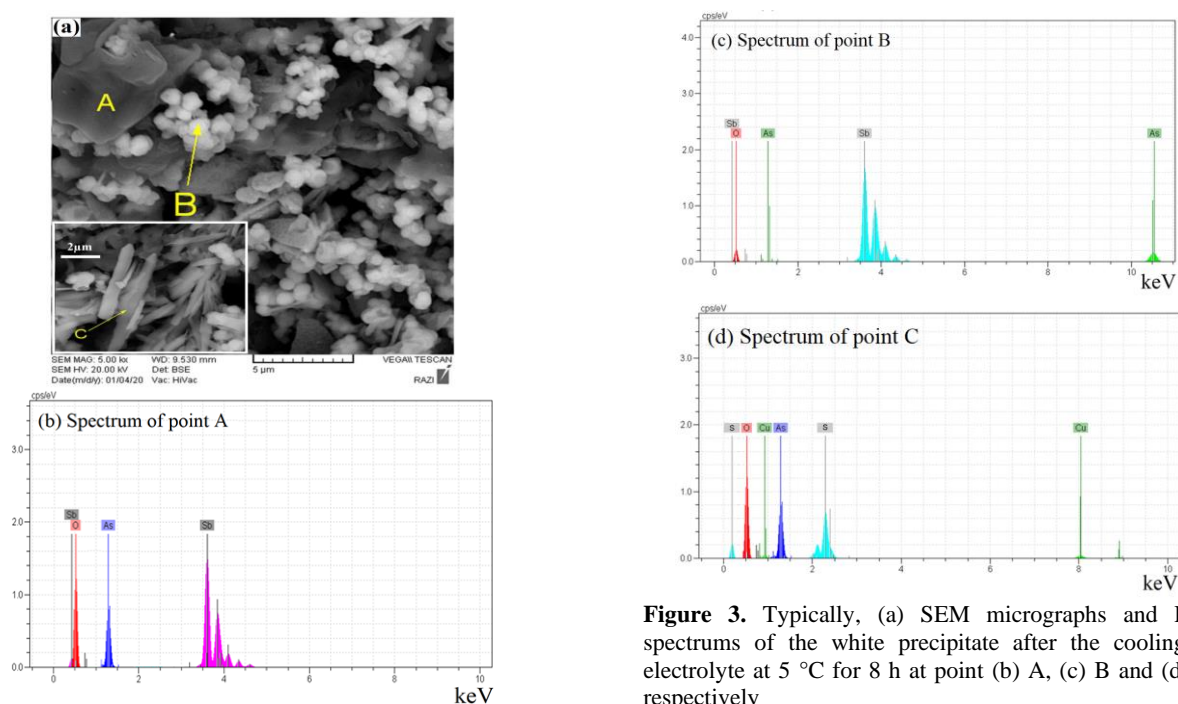
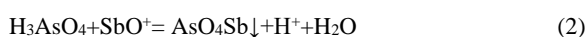


Figure 3. Typically, (a) SEM micrographs and EDS spectra of the white precipitate after the cooling of electrolyte at 5 °C for 8 h at point (b) A, (c) B and (d) C, respectively

TABLE 2. Typically abbreviation of chemical composition of as received electrolyte and cooled electrolyte at 5 °C for 8 h (± 1 ppm or ± 0.001 g/L)

Element/ion	As _t (g/L)	As ⁵⁺ (g/L)	As ³⁺ (g/L)	Sb _t (g/L)	Sb ⁵⁺ (g/L)	Sb ³⁺ (g/L)	Bi (ppm)	Cu (g/L)
As received electrolyte	3.27	3.07	0.20	0.44	0.18	0.26	12	45
After cooling to 5 °C for 8 h	3.07	2.84	0.23	0.32	0.09	0.23	12	45

of its value at 45 °C. Dependency between the temperature and solubility of oxygen is the other factor that must be considered. As a general trend, the solubility of O₂ decreases at the higher temperature. For example, the equilibrium content of O₂ solubility in synthetic electrolyte with 200 g/L H₂SO₄ is to be about 0.72 mM/L at 62 °C and 1.61 mM/L at 5°C [20]. While, in our experiments, due to the lower retention time (8 h) and being stagnant of the electrolyte there is not sufficient time for the diffusion of O₂ from the atmosphere to the electrolyte. Accordingly, from one hand the lower O₂ content of electrolyte respect to the equilibrium amount and on the other hand the higher stability of As(III) respect to As(V) at lower temperature providing a suitable condition for the conversion of As(III) to As(V). Accordingly, by consideration of the results of the XRD spectra as well as the chemical analysis of filtered electrolytes, it can be concluded that the following reactions (Equations (1)-(4)) are responsible for the removal of As and Sb from the electrolyte.



The mixture of AsO₅Sb and AsO₄Sb is formed and deposits according to reactions (1) and (2). Moreover, the cooling of the electrolyte promoted the reduction of As(V) to As(III) [21] as shown in reaction 3. Then, some amount of As(III) ion oxidized by dissolved oxygen in the electrolyte and produce As₂O₃ as precipitate (reaction 4). Wang et al. [22] proposed that the formation AsO₄Sb as the white powder is possible through the cooling of copper refining electrolyte.

3. 4. Molecular Structures of the Formation Phases

The optimized geometry of the structures is shown in Figure 4. Accordingly, three structures can be considered for As₂O₃. Since, the structure of As₂O₃⁻² in Figure 4(b) has the lowest total energy, it is more probable that this structure is formed. The total energies of the three structures of As₂O₃ are shown in Table 3.

The highest occupied molecular orbital (HOMO) isosurfaces of each structure are shown in Figure 5. For

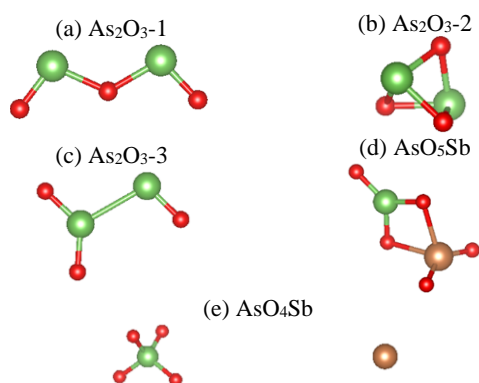


Figure 4. The optimized structures of observed phases including (a-c): As_2O_3 , (d): AsO_5Sb and (e): AsO_4Sb

TABLE 3. Total energies of the three structure of As_2O_3

Structures of As_2O_3	Energy (kJ/mol)
1	-159102.466
2	-159166.75
3	-158953.023

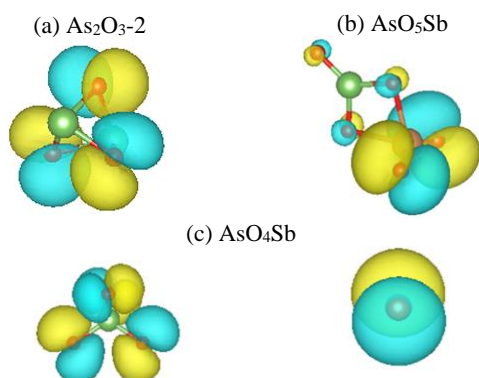


Figure 5. HOMO isosurfaces of the formation phases obtained from DFT calculations

each structure, the HOMO energy levels are mostly localized on oxygen atoms of the structures and have a negligible portion on As and Sb except for AsO_4Sb . This may be indicative of the ionic nature of the structures in which the most of the electron sharing is from As and Sb atoms. Also, for AsO_4Sb structure, the Sb atom is about 12 Å further from the AsO_4 in the simulation cell, which again shows the ionic nature of the structure.

3. 5. FTIR Analysis of White Precipitates

FTIR pattern of the white precipitate is given in Figure 6. There is a vibration bond at 2605.27 cm^{-1} due to the adsorption of CO_2 in the atmosphere to the precipitate. The bond at 1287.43 , 1013.84 , 1071.65 and 1175.67 cm^{-1} are the bending vibration absorption spectrum of As-OH [23-

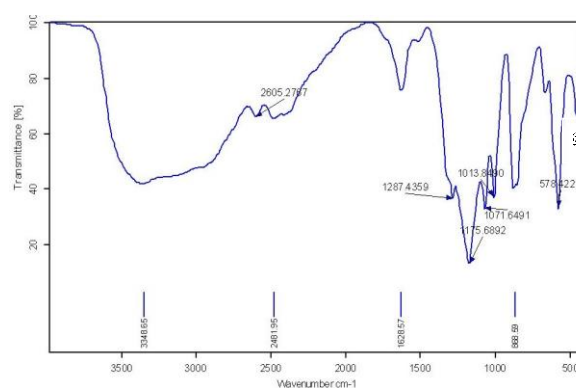


Figure 6. FTIR spectrum of white precipitate that collected from cooled electrolyte at $5\text{ }^\circ\text{C}$ for 8 h

25], the bond at 868.59 cm^{-1} is the anti-stretching vibration absorption spectrum of As-O-Sb and/or As-O-As [26]. The bond at 1287.44 , 878.42 , 1628.57 and 1175.69 cm^{-1} are the anti-stretching vibration absorption spectrum of Sb-OH [23-25], and the bond at 578.42 cm^{-1} is the anti-stretching vibration absorption spectrum of Sb-O-As [27-29], and the bend at 3348.65 and 1628.27 cm^{-1} are the bending vibration absorption spectrum of O-H [23, 24]. The bond at 450.10 cm^{-1} is inferred as the bending vibration absorption spectrum of O-As-O [26]. The presence of these valence bonds confirms the results of the XRD.

4. CONCLUSION

In this study, a green approach is proposed for selective removal of Sb and As from the electrolyte of copper the electrorefining plant. Experimental results showed that the cooling of industrial electrolyte is able to remove about 27 wt.% of Sb, 6 wt.% of As(V) and reactivation of 1 wt.% of As(v) to As(III) by effecting on the solubility of As(V), As(III), Sb(III) and Sb(V). Removing of these impurities is done by the formation of As_2O_3 , AsO_5Sb and AsO_4Sb as white precipitates. The results confirm the need for the storage of electrolyte at any selected temperature for a specified period. Longer storage time results in the precipitation of copper as blue copper sulfates on the primary white precipitate. Accordingly, an efficient approach proposed without using an organic solvent, expensive the raw materials, and complicated equipments for selective removal of Sb and As from the industrial electrolyte.

5. REFERENCES

- Schlesinger, M. E., Sole, K. C., & Davenport, W. G., "Extractive metallurgy of copper", *Elsevier*, Fourth ed., , 2011.

2. Artzer, A., Moats, M. & Bender, "Removal of Antimony and Bismuth from Copper Electrorefining Electrolyte: Part I—A Review", *Jom*, Vol. 70, No. 10, (2018), 2033-2040. <https://doi.org/10.1007/s11837-018-3075-x>
3. Artzer, A., Moats, M., & Bender, "Removal of Antimony and Bismuth from Copper Electrorefining Electrolyte: Part II—An Investigation of Two Proprietary Solvent Extraction Extractants", *Jom*, Vol.70, No. 12, (2018), 2856-2863. <https://doi.org/10.1007/s11837-018-3129-0>
4. Acharya, S., "Copper Refining Electrolyte and Slime Processing-Emerging Techniques", *In Advanced Materials Research*, Vol. 828, (2014), 93-115. <https://doi.org/10.4028/www.scientific.net/AMR.828.93>
5. Zeng, W., Wang, S., & Free, M., L., "Experimental studies of the effects of anode composition and process parameters on anode slime adhesion and cathode copper purity by performing copper electrorefining in a pilot-scale cell", *Metallurgical and Materials Transactions B*, Vol. 47, No. 5, (2016), 3178-3191. <https://doi.org/10.1007/s11663-016-0736-4>
6. Navarro, P., Simpson, J., & Alguacil, F., "Removal of antimony (III) from copper in sulphuric acid solutions by solvent extraction with LIX 1104SM", *Hydrometallurgy*, Vol. 53, No. 2, (1999), 121-131. [https://doi.org/10.1016/S0304-386X\(99\)00033-X](https://doi.org/10.1016/S0304-386X(99)00033-X)
7. Hyvarinen, O., V., 1979. P. *U.S. Patent*, No. 4,157,946. Washington, DC: U.S. Patent and Trademark Office.
8. Wang, X., Wang, X., Liu, B., Wang, M., Wang, H., Liu, X., & Zhou, S., "Promotion of copper electrolyte self-purification with antimonic oxides", *Hydrometallurgy*, Vol. 175, (2018), 28-34. <https://doi.org/10.1016/j.hydromet.2017.10.028>
9. Nie, H., Cao, C., Xu, Z., & Tian, "Novel method to remove arsenic and prepare metal arsenic from copper electrolyte using titanium (IV) oxysulfate coprecipitation and carbothermal reduction", *Separation and Purification Technology*, Vol. 231, (2020), 115919. <https://doi.org/10.1016/j.seppur.2019.115919>
10. Xiao, F. X., Dao, C. A. O., Mao, J. W. Shen, X. N. & Ren, F. Z., "Role of Sb (V) in removal of As, Sb and Bi impurities from copper electrolyte", *Transactions of Nonferrous Metals Society of China*, Vol. 24, (2014), 271-278. [https://doi.org/10.1016/S1003-6326\(14\)63057-0](https://doi.org/10.1016/S1003-6326(14)63057-0)
11. Stantke, P., "Using CollaMat to measure glue in copper electrolyte", *JOM*, Vol.54, (2002), 19-22.
12. Hutter, J., Iannuzzi, M., Schiffrmann, F., & VandeVondele, "CP2K: atomistic simulations of condensed matter systems. Wiley Interdisciplinary Reviews", *Computational Molecular Science*, Vol. 4, (2014), 15-25. <https://doi.org/10.1002/wcms.1159>
13. V., Vondele, J. & Hutter, "Gaussian basis sets for accurate calculations on molecular systems in gas and condensed phases", *Chemical Physics*, Vol. 127, No. 11, (2007), 114105. <https://doi.org/10.1063/1.2770708>
14. Perdew, J., P., Burke, K., & Ernzerhof, M., "Generalized gradient approximation made simple", *Physical Review Letters*, Vol. 77, (1996), 3865.
15. Goedecker, S., Teter, M., & Hutter, "Separable dual-space Gaussian pseudopotentials", *Physical Review B*, Vol. 54, (1996), 1703. <https://doi.org/10.1103/PhysRevB.54.1703>
16. Press, W. H., Teukolsky, S. A., Vetterling, W. T., & Flannery, B. P., "Numerical recipes 3rd edition: The art of scientific computing. Third ed", *Cambridge University Press*, 2007.
17. Momma, K., & Izumi, F., "VESTA 3 for three-dimensional visualization of crystal, volumetric and morphology data", *Applied Crystallography*, Vol. 44, (2011), 1272-1276. <https://doi.org/10.1107/S0021889811038970>
18. Xiao, F., X., Cao, D., Mao, J., W., & Shen, X., N., "Mechanism of precipitate removal of arsenic and bismuth impurities from copper electrolyte by antimony", *In Advanced Materials Research*, Vol. 402, (2012), 51-56. <https://doi.org/10.4028/www.scientific.net/AMR.402.51>
19. Peng, Y., L., Zheng, Y., J., & Chen, W., M., "The oxidation of arsenic from As (III) to As (V) during copper electrorefining", *Hydrometallurgy*, Vol. 129, (2012), 156-160. <https://doi.org/10.1016/j.hydromet.2012.06.009>
20. Xing, W., Yin, G., & Zhang, J., "Rotating electrode methods and oxygen reduction electrocatalysts. Elsevier, Fourth (Ed.), (2014).
21. Jergensen, G. V., "Copper leaching", *Solvent Extraction, and Electrowinning Technology*, Third (Ed.) SME, (1999).
22. Xue-Wen, W., Qi-Yuan, C., Zhou-Lan, Y., & Lian-Sheng, X., "Identification of arsenato antimonates in copper anode slimes", *Hydrometallurgy*, Vol. 84, (2006), 211-217. <https://doi.org/10.1016/j.hydromet.2006.05.013>
23. Naili, H., & Mhiri, T., "X-ray structural, vibrational and calorimetric studies of a new rubidium pentahydrogen arsenate $RbH_5(AsO_4)_2$ ", *Alloys and Compounds*, Vol. 315, (2001), 143-149. [https://doi.org/10.1016/S0925-8388\(00\)01309-8](https://doi.org/10.1016/S0925-8388(00)01309-8)
24. Qureshi, M., & Kumar, V., "Synthesis and IR, X-ray and ion-exchange studies of some amorphous and semicrystalline phases of titanium antimonate: separation of VO^{2+} from various metal ions", *Chromatography A*, Vol. 62, (1971), 431-438. [https://doi.org/10.1016/S0021-9673\(00\)91395-5](https://doi.org/10.1016/S0021-9673(00)91395-5)
25. Colomban, P., Doremieux-Morin, C., Piffard, Y., Limage, M. H., & Novak, A., "Equilibrium between protonic species and conductivity mechanism in antimonic acid, $H_2Sb_4O_{11} \cdot nH_2O$ ", *Journal of Molecular Structure*, Vol. 213, (1989), 83-96. [https://doi.org/10.1016/0022-2860\(89\)85108-7](https://doi.org/10.1016/0022-2860(89)85108-7)
26. Zongsheng, Z., "Mechanism of arsenic removal in oxidized Fe-As system". *Journal of China Environmental Science*, Vol. 1, (1995).

Persian Abstract

چکیده

حذف آرسنیک و آنتیموان از طریق سردسازی الکترولیت صنعتی کارخانه پالایش الکتریکی مس صورت گرفت. به عنوان یک مسیر نوین، در پژوهش حاضر، دمای الکترولیت به 5، 10، 15 و 20 درجه سانتی گراد کاهش یافته و در زمان های مختلف بدون تلاطم نگهداری گردید. نتایج تجربی نشان می دهد که کاهش دمای الکترولیت، رسوب As و Sb را به شکل As_2O_3 و AsO_4Sb ، AsO_5Sb به عنوان رسوب سفید در یک زمان بحرانی بوجود می آورد. همچنین، در مواردی که زمان نگهداری الکترولیت در دماهای مذکور بیشتر از زمان بحرانی باشد، محتوای مس الکترولیت به صورت فاز آبی رسوب می کند. به عنوان مثال، می توان 27 درصد وزنی Sb و 6 درصد وزنی As را با خنک سازی الکترولیت تا 5 درجه سانتیگراد پس از 8 ساعت حذف کرد. به نظر می رسد با توجه به سازگاری زیست محیطی، عدم نیاز به فنآوری پیچیده و سادگی، روش پیشنهادی جایگزین مناسبی برای روش های رایج برای از حذف آنتیموان و آرسنیک در مقیاس صنعتی باشد.
